Supporting Online Material for

Eliminating Turbulence in Spatially Intermittent Flows

Björn Hof,* Alberto de Lozar, Marc Avila, Xiaoyun Tu, Tobias M. Schneider

*To whom correspondence should be addressed. E-mail: bhof@gwdg.de

Published 19 March 2010, *Science* **327**, 1491 (2010)
DOI: 10.1126/science.1186091

This PDF file includes:

Other Supporting Online Material for this manuscript includes the following:
(available at www.sciencemag.org/cgi/content/full/327/5972/1491/DC1)

Eliminating turbulence in spatially intermittent flows

Supporting online materials

Björn Hof[1]†, Alberto de Lozar[1], Marc Avila[1], Xiaoyun Tu[1,2] and Tobias M. Schneider[3]

[1]*Max Planck Institute for Dynamics and Self-Organisation, Bunsenstrasse 10, 37073 Göttingen, Germany*

[2]*Present address: LaVision GmbH, Göttingen, Germany*

[3]*School of Engineering and Applied Sciences, Harvard University, 29 Oxford Street, Cambridge, MA 02138, USA*

1. Vortex regeneration and inflectional instability.

A turbulent puff has been simulated numerically at Re=1900[i] (details of the numerical scheme are given in section 2). As discussed in the main part of the paper the turbulence regeneration cycle comprises upstream travelling (relative to the puff speed) vortices that continuously distort the laminar fluid in the near wall region (L/D<0 in Fig. 1C, where L is the axial position). In doing so, they sustain the inflection points which in turn cause the instability (located at L/D=0) that regenerates vorticity.

To locate the inflectional instability curvature changes of the azimuthally averaged velocity profiles were determined at each axial position. Since the second derivative of the parabolic laminar profile, $u_p(r)''$ (here ' denotes the radial derivative and r the radial coordinate, u is the axial velocity component and the subscript p denotes the parabolic laminar flow) is negative ($u_p(r)''= (1-r^2)''=-2$), $u(r)''$ has to become positive at an inflection point. In order to quantify the magnitude of curvature at the

[i] The Reynolds number is here defined as Re= ŪD/ν, where Ū is the mean flow speed, D the pipe diameter and ν the kinematic viscosity.

inflection point we summed over positive values of u(r)'' on the radial interval 0.6<r<0.8. This interval was chosen following earlier studies (*21*, *S1*), where it has been shown that the most sensitive radial location for an inflectional disturbance of the laminar profile is at r≈0.7. At the same time the vorticity transport, $<|\omega_z|,u-\bar{U}>$, was calculated (ω_z denotes the axial component of the vorticity) for each axial position and the zero crossing of this quantity determined the vorticity source. Based on this location the vorticity transport, the inflection point amplitude as well as the turbulent kinetic energy were time averaged over 70 dimensionless time units.

Also, to simplify the analysis, we looked for inflection points in the azimuthally averaged profiles. This quantity has a distinct peak (red curve in Fig. S1) at the axial location of L/D=0, where also axial vorticity is created (zero crossing of black curve in Fig. S1). As shown in reference 21 (Figure 18), even weak inflection points render the parabolic flow unstable and the proceeding instability leads to the production of axial vorticity and eventually triggers turbulence.

A non-averaged velocity profile at the axial location of the strongest inflection point is shown in Fig. S1. The streamwise velocity is represented by the color scale and in plane motion by the velocity vectors. The azimuthal location with the strongest inflection point is marked by the solid black line. The particular aspect of this location is that the high speed region close to the wall is followed (in the radial direction) by a low speed region. As shown in Fig. S1 B the inflection point hence produces a local minimum in the velocity profile. Also note that the strong vortex, creating this imbalance of the profile, travels upstream (i.e. slower than the inflection point) when viewed in a commoving frame.

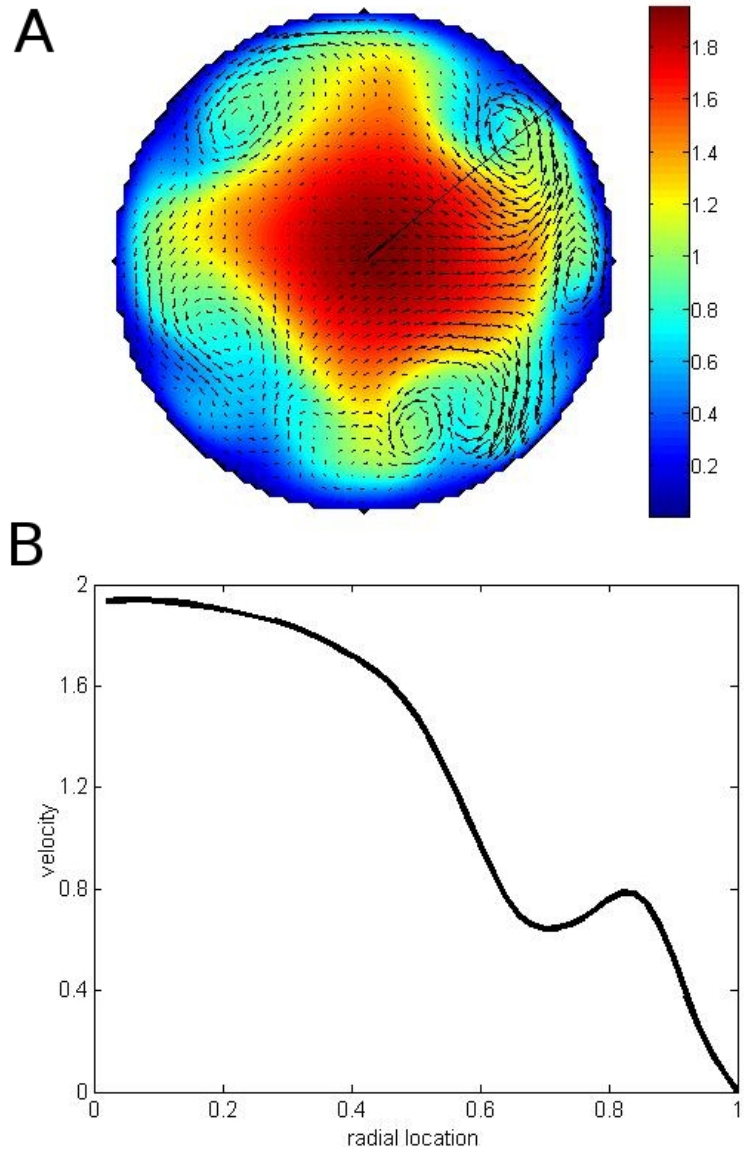

Fig. S1: A: Contour plot of velocity profile at the axial location with the strongest inflection point, corresponding to the instant plotted in Fig. 3B (fourth panel from the left). The strongest inflection point is found at the location marked by the black line and shown in B. The radial location =0 corresponds to the pipe centre.

2. Numerical formulation

We consider an incompressible viscous fluid which is driven through a circular pipe at a constant flow rate. The motion of the fluid is governed by the incompressible Navier–Stokes equations

$$\partial_t \mathbf{v} + (\mathbf{v}\cdot\nabla)\mathbf{v} = -\nabla p + \frac{4}{\mathrm{Re}}(1+\beta)\hat{\mathbf{z}} + \frac{1}{\mathrm{Re}}\Delta\mathbf{v} + \mathbf{F}, \quad \nabla\cdot\mathbf{v} = 0\,, \qquad (1)$$

where v is the velocity vector field, β is the additional pressure gradient fraction required to maintain the flow-rate constant and **F** an applied volume force. Note that the Reynolds number based on the pressure gradient is $\mathrm{Re}_p = (1+\beta)\mathrm{Re}$, i.e. in the case of laminar flow β = 0. The equations have been non-dimensionalized with D/2 for space and 2 $\bar{U}$ for velocity. The boundary conditions are no-slip at the pipe wall, whereas v is assumed periodic in the axial direction. In order to properly simulate turbulent puffs, a long periodic domain of length Λ = 50D has been used in the present computations. This is sufficient to avoid the interaction between leading and trailing edge of the localized structure of a puff which would arise in short domains. The geometry of the system is exploited in the formulation of the problem via cylindrical coordinates (r, θ, z). We employ a spectral Petrov–Galerkin approach which efficiently resolves the difficulties arising from the Navier–Stokes equations in cylindrical geometries. The velocity field v is represented as

$$\mathbf{v}(r,\theta,z,t) = v_P(r)\hat{\mathbf{e}}_z + \mathrm{Real}[\sum_{l=-L}^{L}\sum_{n=-N}^{N}\sum_{m=0}^{M} a_{lnm}(t)\mathrm{e}^{\mathrm{i}(2\pi l/\Lambda z + n\theta)}\mathbf{u}_{lnm}(r)], \qquad (2)$$

where $v_P(r) = 1-r^2$ is the parabolic Poiseuille profile. Details on the formulation of the method, as well as extensive convergence tests, can be found in (*S2, S3*). Here, a numerical resolution of (L,N,M) = (446, 26, 44) has been used resulting in well resolved solutions of the Navier–Stokes equations.

3. Forcing the laminar profile

The stability of turbulent puffs is influenced by applying a forcing term F to the Navier–Stokes equations (1). The presence of a non-zero F in the equations modifies its underlying solutions, resulting in non-parabolic stream-wise basic velocity profiles. Thus, one can systematically investigate the effect of modified profiles in the stability of turbulent puffs. Consider a family of forcings F(r, α) that modify the

laminar parabolic profile by accelerating the fluid close to the pipe-wall. As a consequence, the velocity of the core must decrease when the mean flow speed is kept constant.

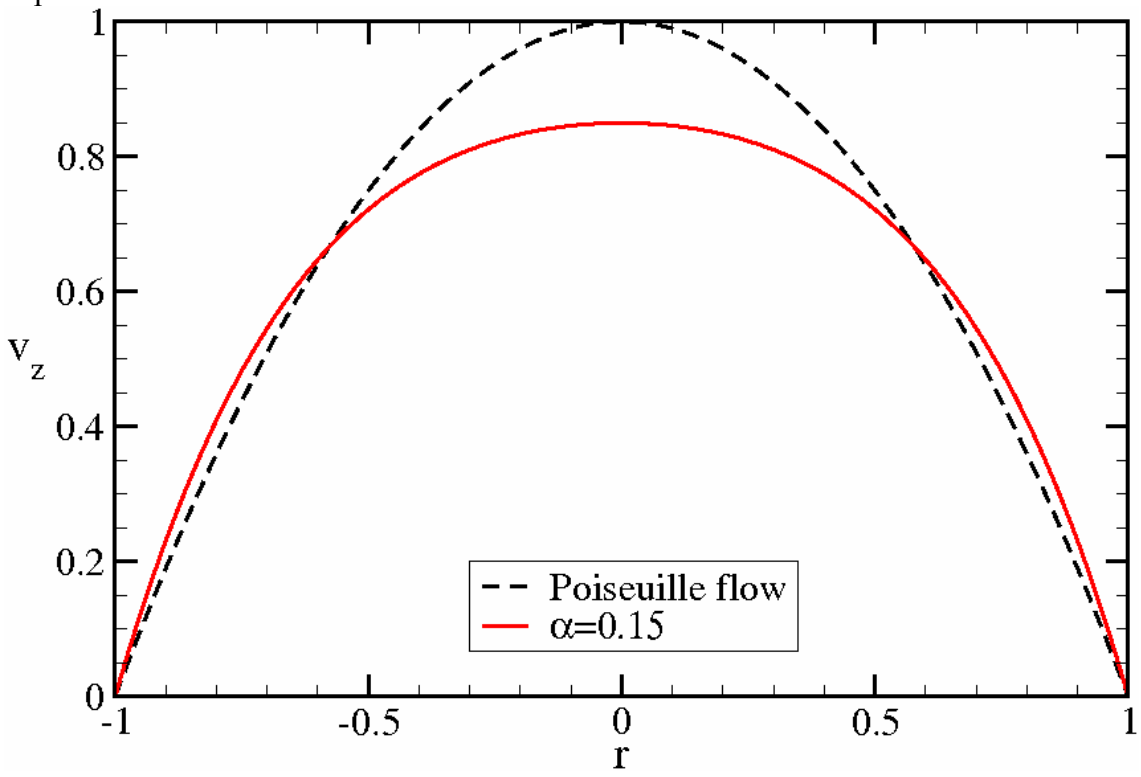

Fig. S2: Laminar Poiseuille profile (dashed line) and forced pluck-like profile, with $\alpha = 0.15$, i.e with a centerline velocity drop of about 15%.

The drop in centerline velocity of the resulting profile with respect to the parabolic Poiseuille profile is controlled by the parameter α. Fig. S2 shows a forced profile (red solid line) with a centerline velocity drop of 15%, i.e. with $\alpha = 0.15$. The parabolic Poiseuille profile, corresponding to $\alpha = 0$, is shown (black dashed line) for comparison. As one is interested in modifying only the stream-wise velocity profile behind a turbulent puff, spatial dependence on the axial direction must be introduced in the forcing term $F = F(r, z, \alpha)$. A Gaussian function $\exp[-((z - z0)/H)^2]$ is used in order to obtain a modified profile which is localized about z0 and has a spatial extent given by H. Further, the location of the forcing can be continuously changed in time $z_0 = z_0(t)$ in order to follow the motion of a turbulent puff as it propagates downstream. For the control simulation shown in Fig. 2 of the paper, we use $\alpha = 0.1$ and the center the forcing at a z_0 which is located slightly behind the vorticity source

of the puff. The spatial extent of the forcing is such that at 3.5D from z_0, there is a factor of 3 drop in strength (corresponding to H≈7D). The forcing is co-moved at a constant speed of c = 1.05Ū, which is the mean propagating speed of a puff at Re = 1900 (*S4*). Details of the method to generate the forcing and extensive systematic testing of the governing parameters will be disseminated separately.

4. Forcing at higher Re

Beyond the intermittent regime (Re~>2500 in pipes) turbulence starts to spread and eventually fills the entire numerical domain. In the numerical simulations the same type of forcing, now extending over the entire numerical domain is still found to be effective and eliminate turbulence (see Fig. S3). The cost of the forcing is only 40% of the drag reduction obtained.

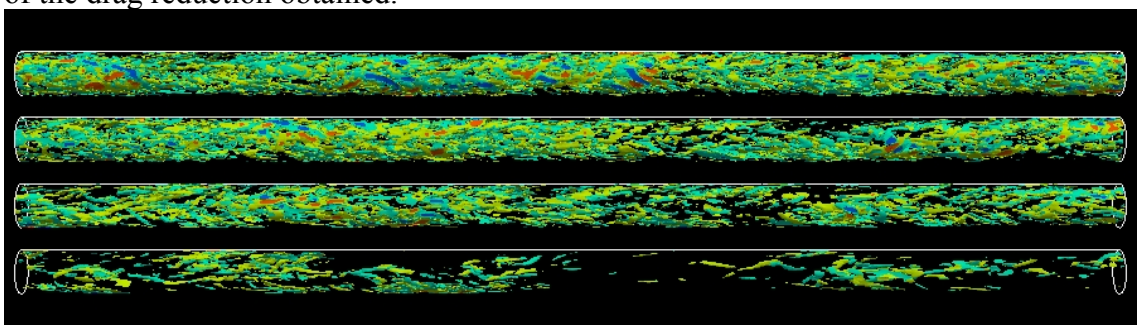

Fig. S3:A forcing with α =0.25 is sufficient to eliminate turbulence in a fully turbulent regime at Re=2900. Snapshots at four different stages after the forcing is applied are shown: t=12.5, t=25, t=37.5 and t=50.

Movie S1: Streamwise vorticity iso-surfaces (positive in blue, negative in red) are viewed in a co-moving frame for pipe flow at Re=1900. The x-axis corresponds to the axial direction and the y-axis to the azimuthal direction (0 to 2π). It is apparent that the vortices are created at a single location x=0. Vortices left of the instability location move downstream and those to the right travel upstream. To improve the visibility of the vortices at x<0, here the amplitude of the streamwise vorticity was multiplied by a factor of 2.5.

References

S1. A.E. Gill, *J. Fluid Mech.* **21**, 503-511 (1965).

S2. A. Meseguer and F. Mellibovsky, *Appl. Num. Math.* **57**, 920-938 (2007).

S3. F. Mellibovsky and A. Meseguer, *Phys. Fluids* **19**, 044102 (2007).

S4. A. de Lozar and B. Hof, *Phil. Trans. R. Soc.* London A **367**, 589–599 (2008).